

GEOSTROPHIC CURRENTS IN THE SOUTH SHETLAND ISLANDS AREA DURING FIBEX

M. STEIN

Institut für Seefischerei, Palmaille 9, D-2000 Hamburg 50, Federal Republic of Germany

and

S. RAKUSA-SUSZCZEWSKI

Institute of Ecology Polish Academy of Sciences, Dziekanów Leśny, 05-150 Lomianki, Poland

Abstract: Based on the Polish/West German FIBEX (First International BIOMASS Experiment) oceanographic data set a description of the kinematic situation in the South Shetland Islands area during February/March 1981 is given. By means of the dynamic topography the distribution of water masses originating from the Bellingshausen Sea and the Weddell Sea, as well as their temporal and spatial changes are discussed.

1. Introduction

At the southern edge of the Drake Passage the archipelago of the South Shetland Islands extends for approximately 500 km in a southwest/northeast direction. Close to the Antarctic Peninsula these islands form a barrier which effectively channels the circumpolar flow of water masses. According to CLOWES (1934), GORDON and NOWLIN (1978) the area between the islands and the Antarctic Peninsula, the Bransfield Strait, is influenced by waters from the Bellingshausen Sea and the Weddell Sea. These water masses penetrate into the Bransfield Strait area from the open boundaries of the strait. From the west Bellingshausen Sea water enters between Low, Smith and Snow Islands. Parts of this current flow north and south of Deception Island where a characteristic bend to the southeast is observed. In the vicinity of Trinity Island the current loops to the northeast and joins the branches at the northern edge of the Bransfield Strait forming a strong flow along the southern coast of the South Shetland Islands. Along the shelf off the Antarctic Peninsula Weddell Sea water influences the southern parts of the strait. The kinematic structure of the Antarctic Circumpolar Current (ACC) between the tips of South America and the South Shetland Islands is given by NOWLIN *et al.* (1977). Based on moored current meter measurements and geostrophic computations they report current bands of high eastward speeds separated by regions of lower speed or even westward flow in the central Drake Passage. Off the north coast of the South Shetland Islands they derive an eastward flow which amounts about 10 cm/s.

At the eastern edge of the South Shetland archipelago a steady flow of about 12 cm/s into 65° was observed by means of moored current meters between the mid of November 1977 and the end of January 1978 (STEIN, 1978). These figures indicate the

order of magnitude of the mean currents north of the islands. They are the only figures on direct measured currents available for the area of the South Shetland Islands. For a description of the circulation patterns in this area one thus has to rely on the indirect methods, *e.g.* the geostrophic method.

During FIBEX the R.V. PROFESSOR SIEDLECKI (Poland), R.V. ITSUMI (Chile) and R.V. WALTHER HERWIG (Federal Republic of Germany) occupied a number of hydrographic stations in the area north and south of the South Shetland archipelago. Based on the Polish and West German oceanographic data the distribution of geostrophic currents in this area is discussed.

2. Data Processing

Between February 15 and March 31, 1981 a total of 118 hydrographic stations were performed by R.V. PROFESSOR SIEDLECKI and R.V. WALTHER HERWIG in the area of the South Shetland Islands (Figs. 2 to 7). These data are part of the Polish/West German FIBEX (First International BIOMASS Experiment) oceanographic data set available in the data base of the Institut für Seefischerei, Hamburg.

Oceanographic Data Base and Data Handling System

Figure 1 outlines the oceanographic data base and the way it is treated by the software. Given a set of n oceanographic stations each of them consisting of station header

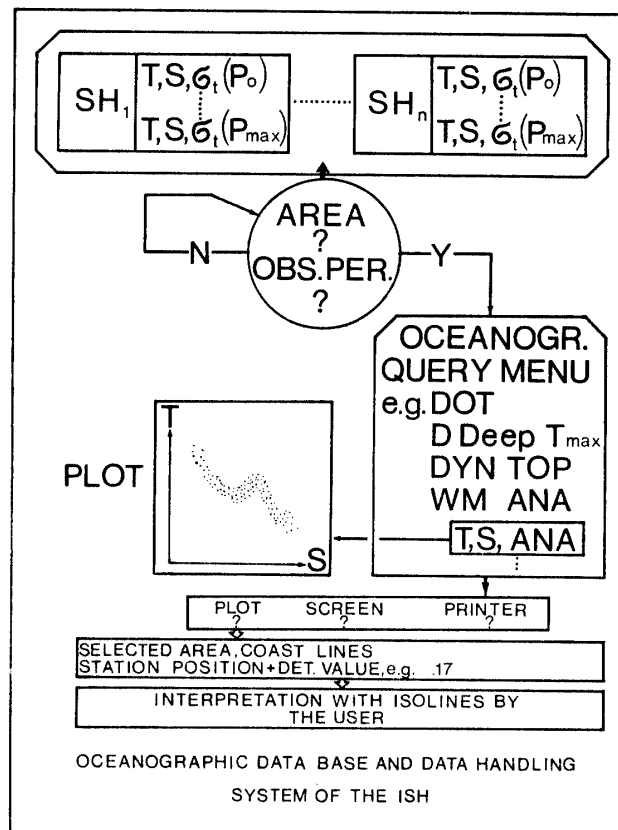


Fig. 1. Oceanographic Data Base and Data Handling System of the ISH.

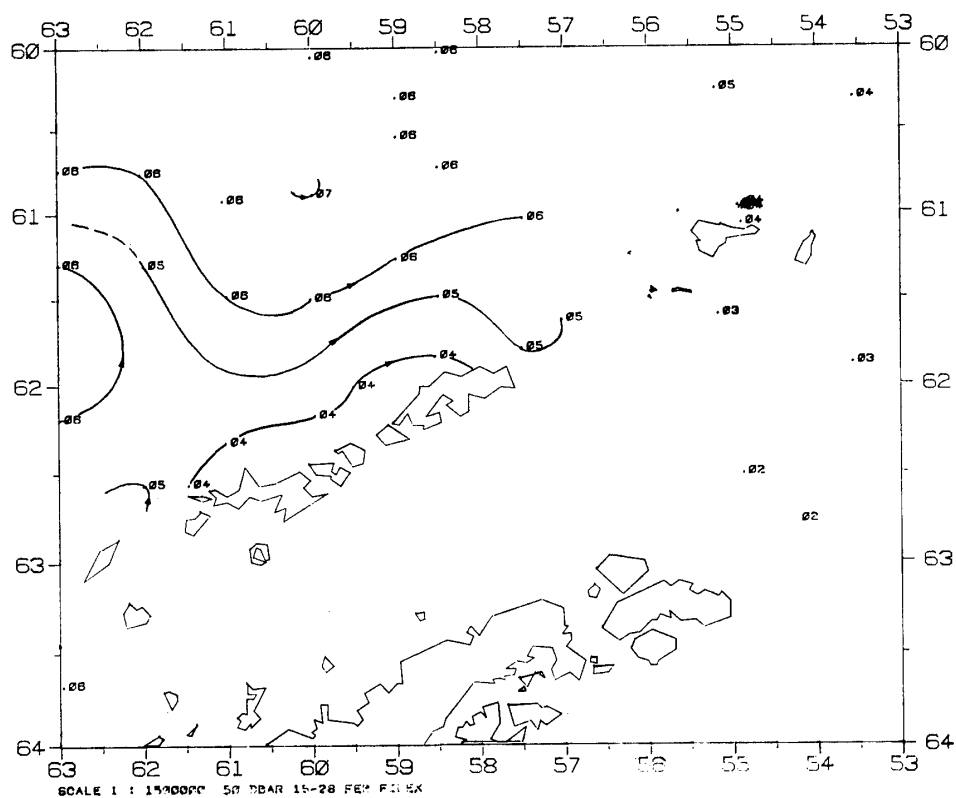


Fig. 2a. Relative dynamic topography of the 50 dbar surface (February 15-28, 1981).

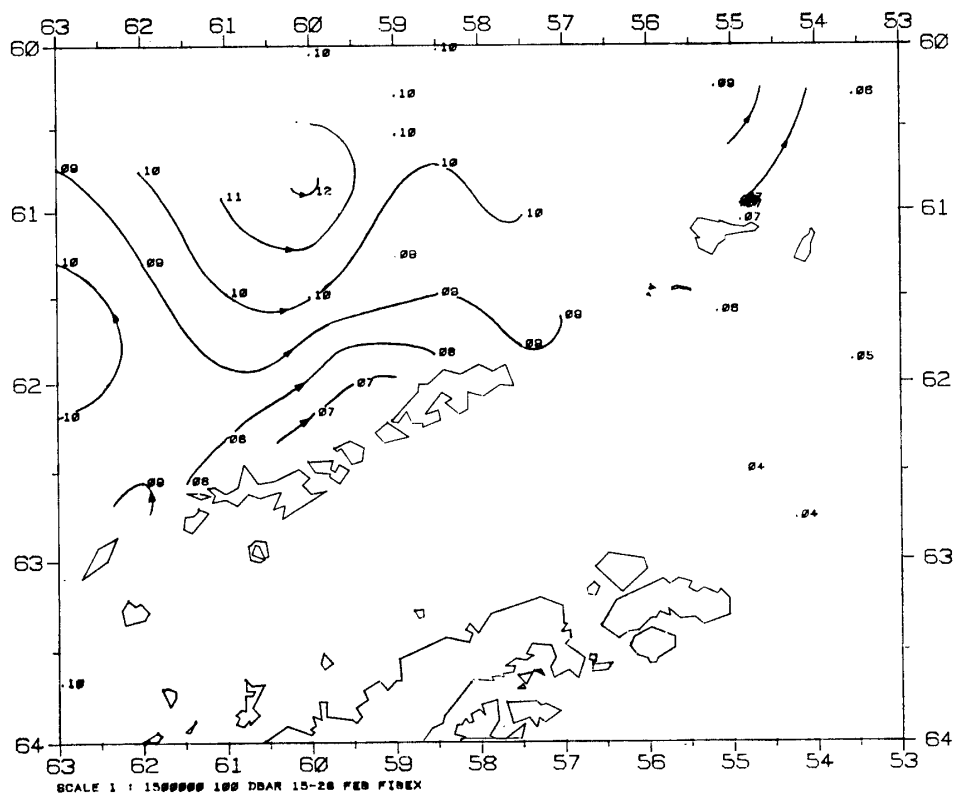


Fig. 2b. Relative dynamic topography of the 100 dbar surface (February 15-28, 1981).

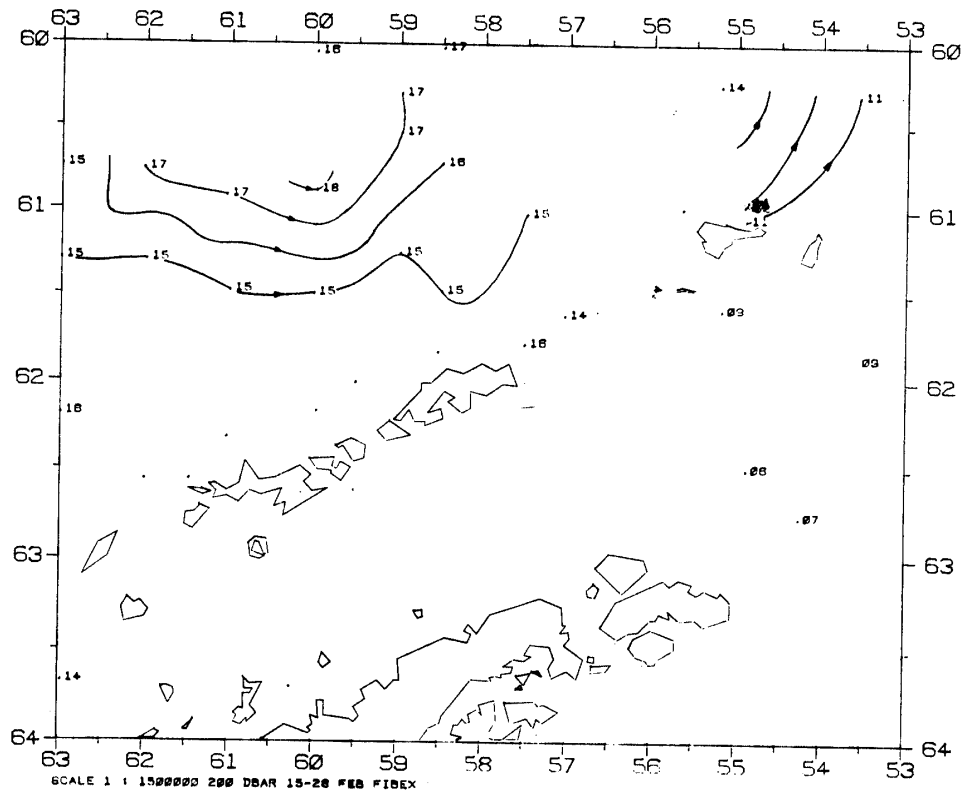


Fig. 3a. Relative dynamic topography of the 200 dbar surface (February 15-28, 1981).

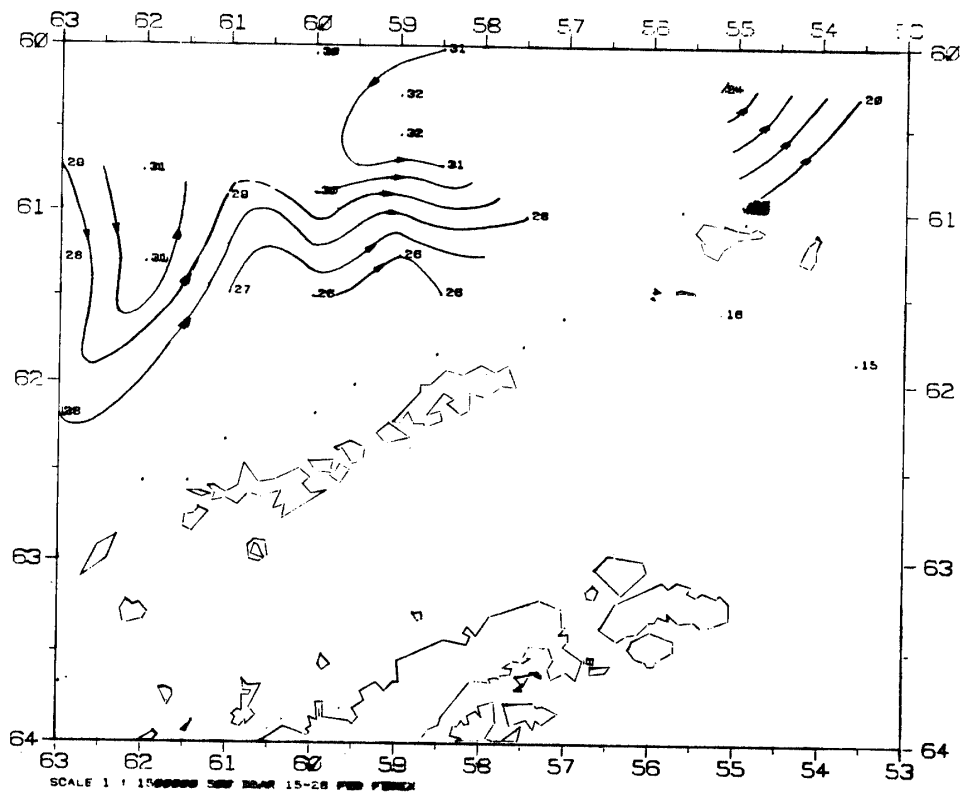


Fig. 3b. Relative dynamic topography of the 500 dbar surface (February 15-28, 1981).

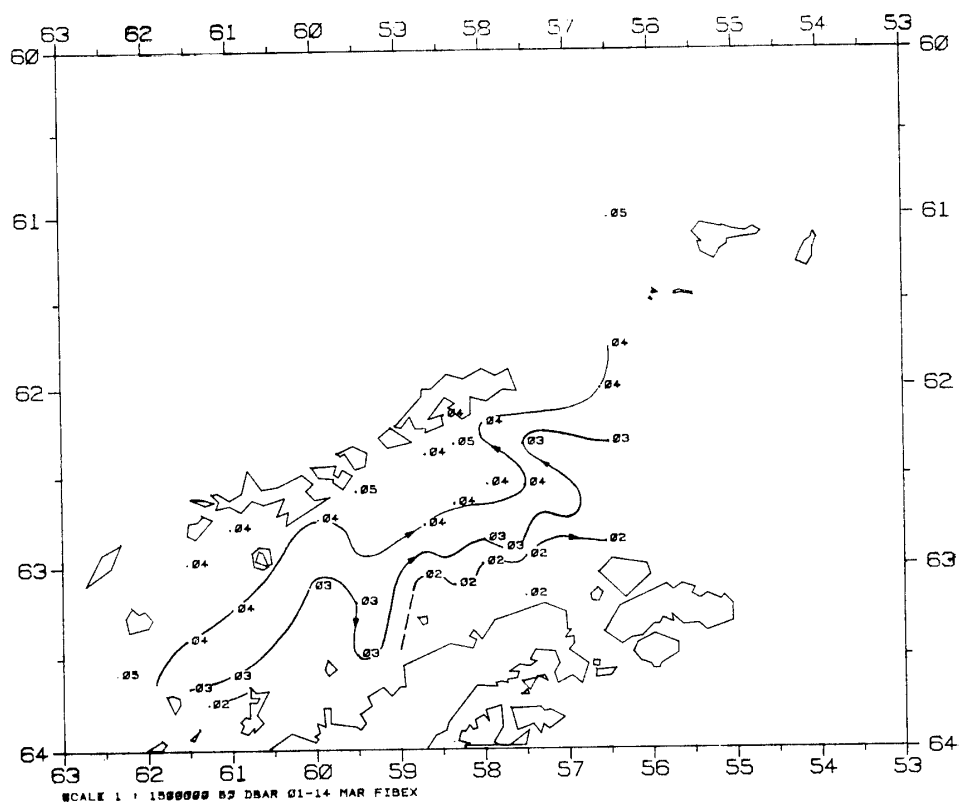


Fig. 4a. Relative dynamic topography of the 50 dbar surface (March 1-14, 1981).

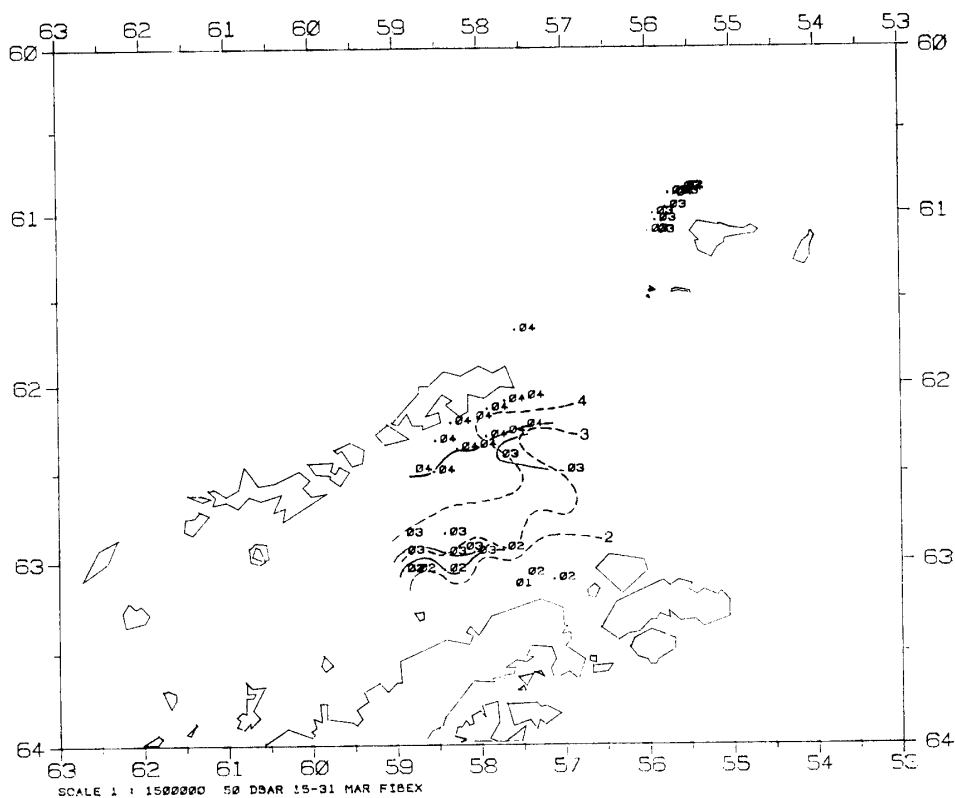


Fig. 4b. Relative dynamic topography of the 50 dbar surface' (March 15-31, 1981).

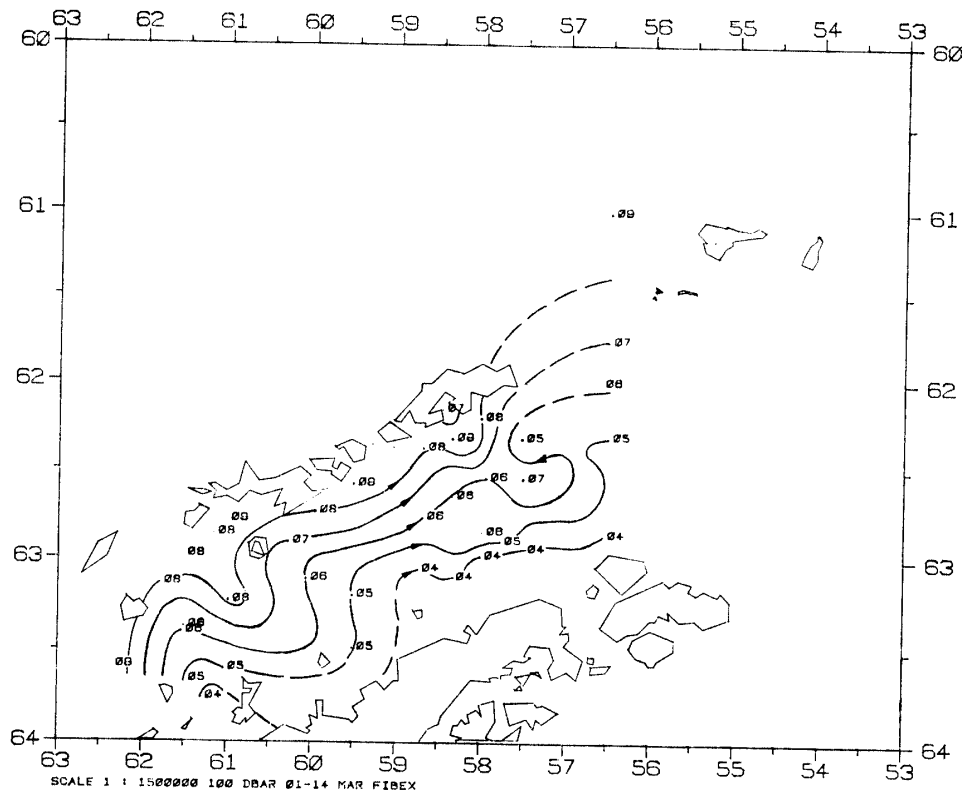


Fig. 5a. Relative dynamic topography of the 100 dbar surface (March 1-14, 1981).

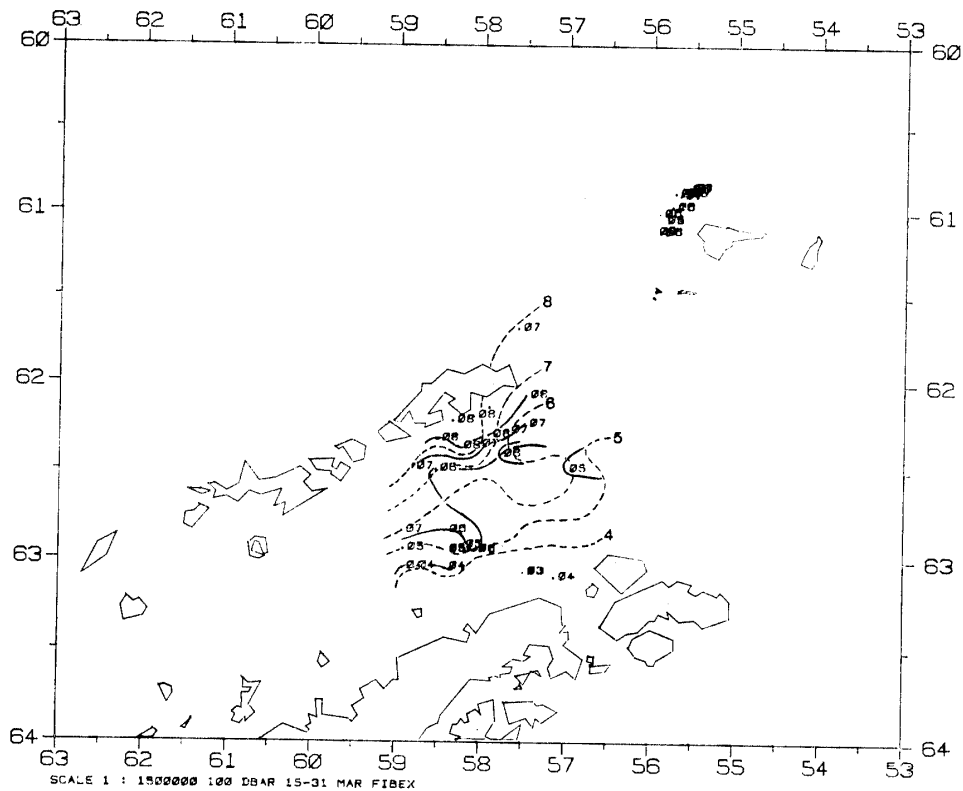


Fig. 5b. Relative dynamic topography of the 100 dbar surface (March 15-31, 1981).

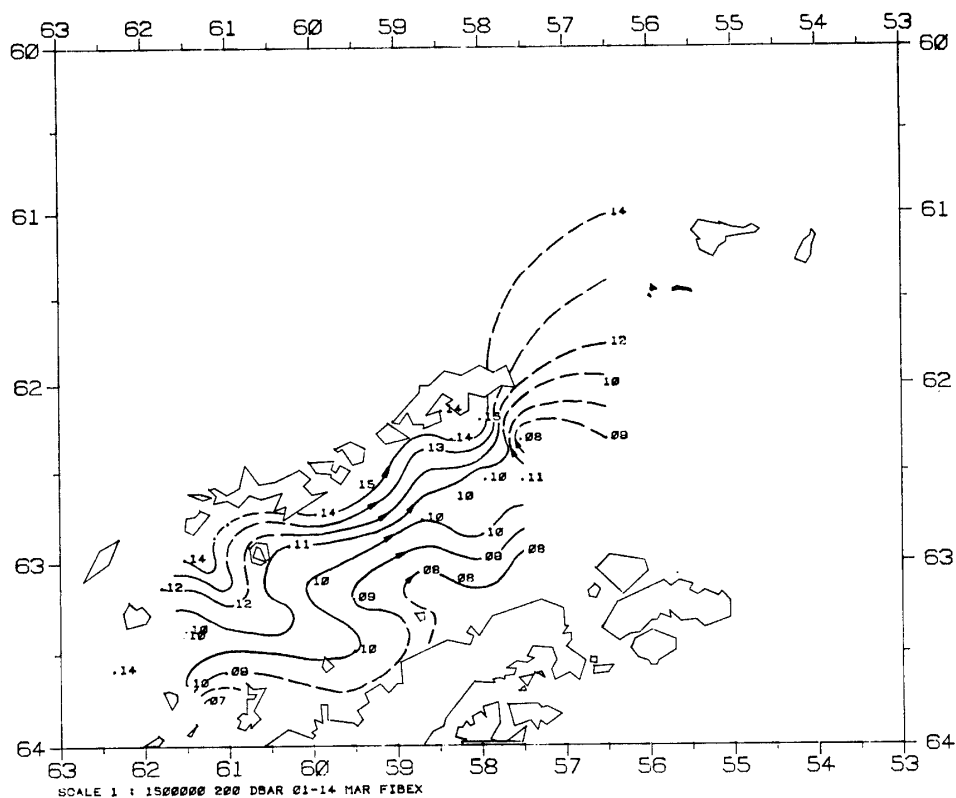


Fig. 6a. Relative dynamic topography of the 200 dbar surface (March 1-14, 1981).

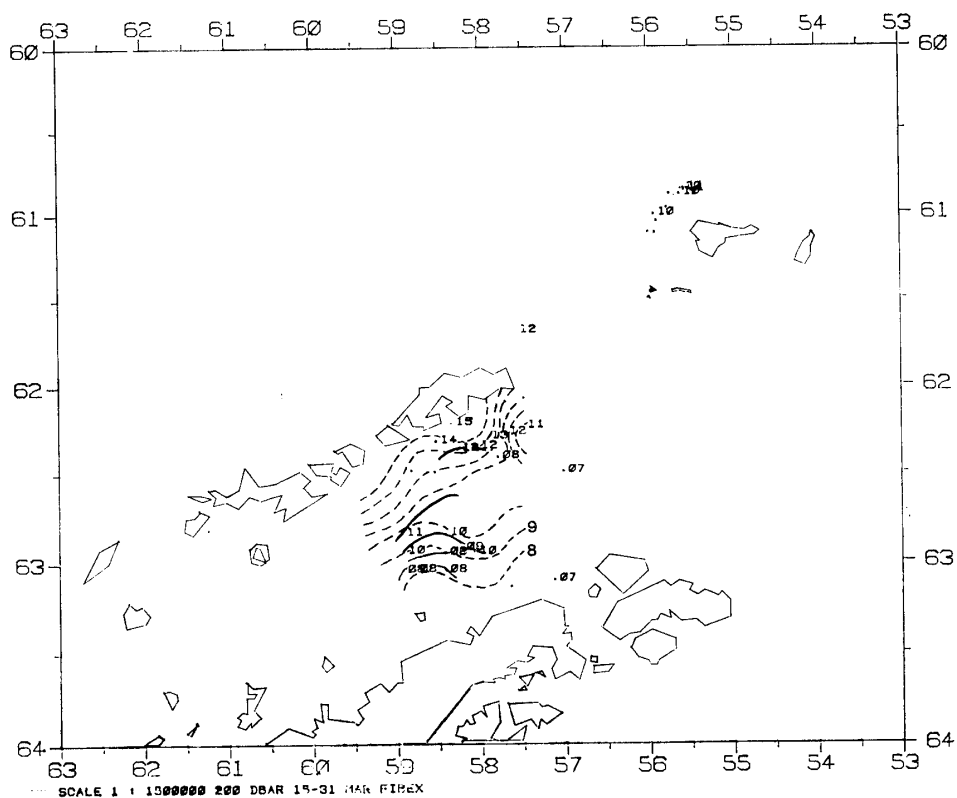


Fig. 6b. Relative dynamic topography of the 200 dbar surface (March 15-31, 1981).

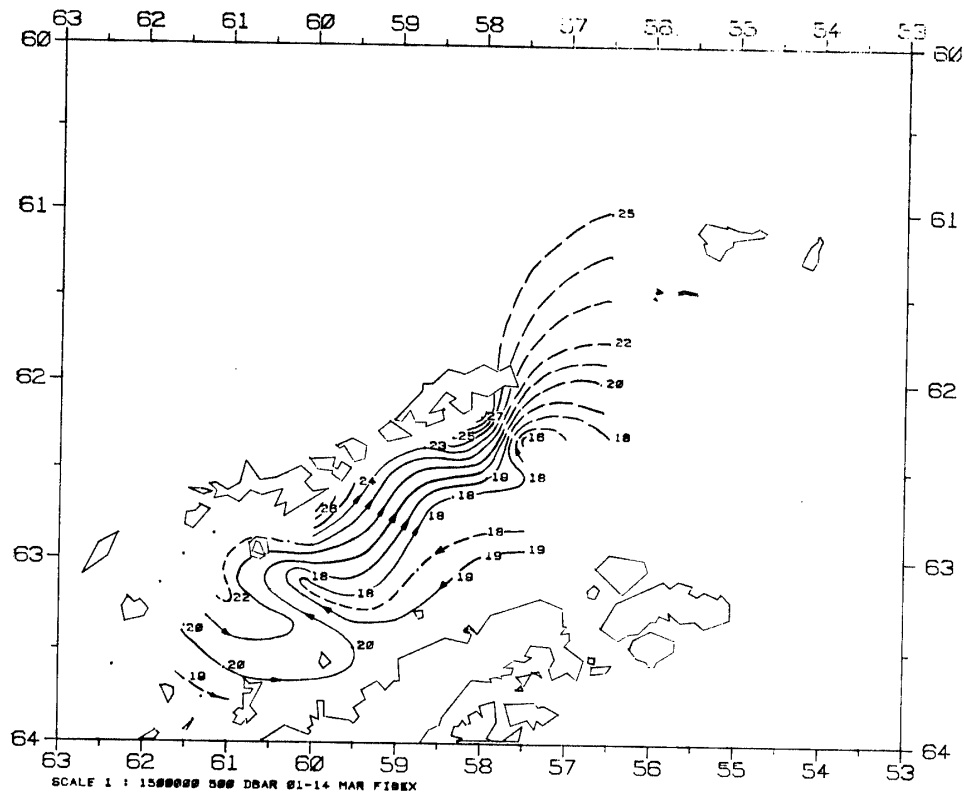


Fig. 7a. Relative dynamic topography of the 500 dbar surface (March 1-14, 1981).

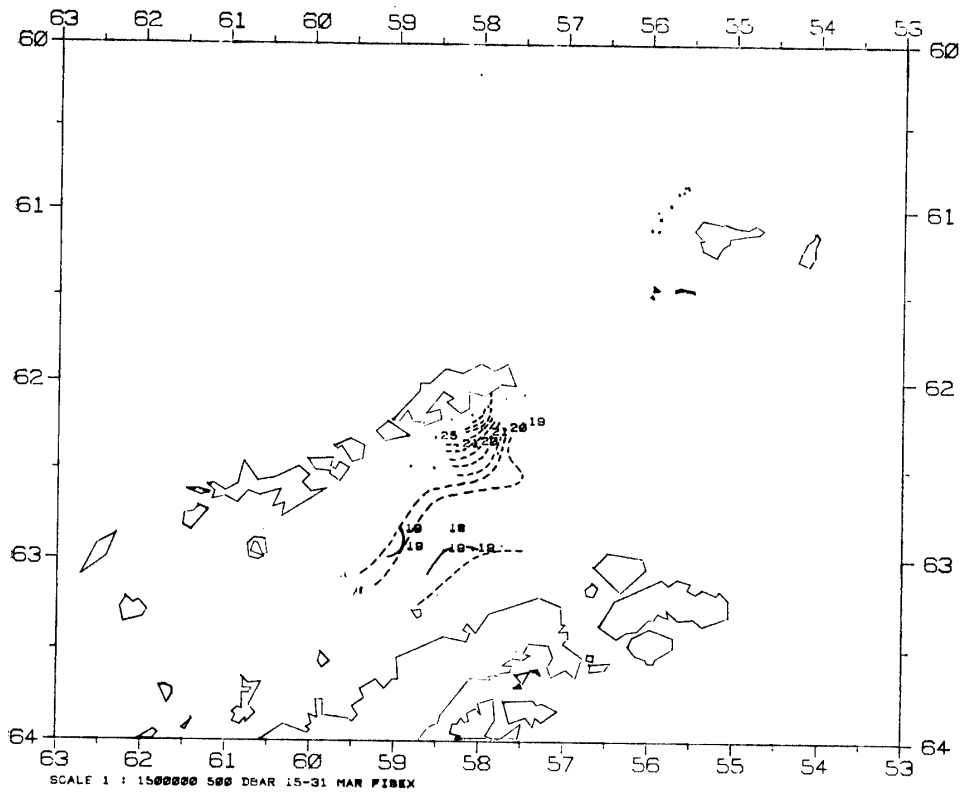


Fig. 7b. Relative dynamic topography of the 500 dbar surface (March 15-31, 1981).

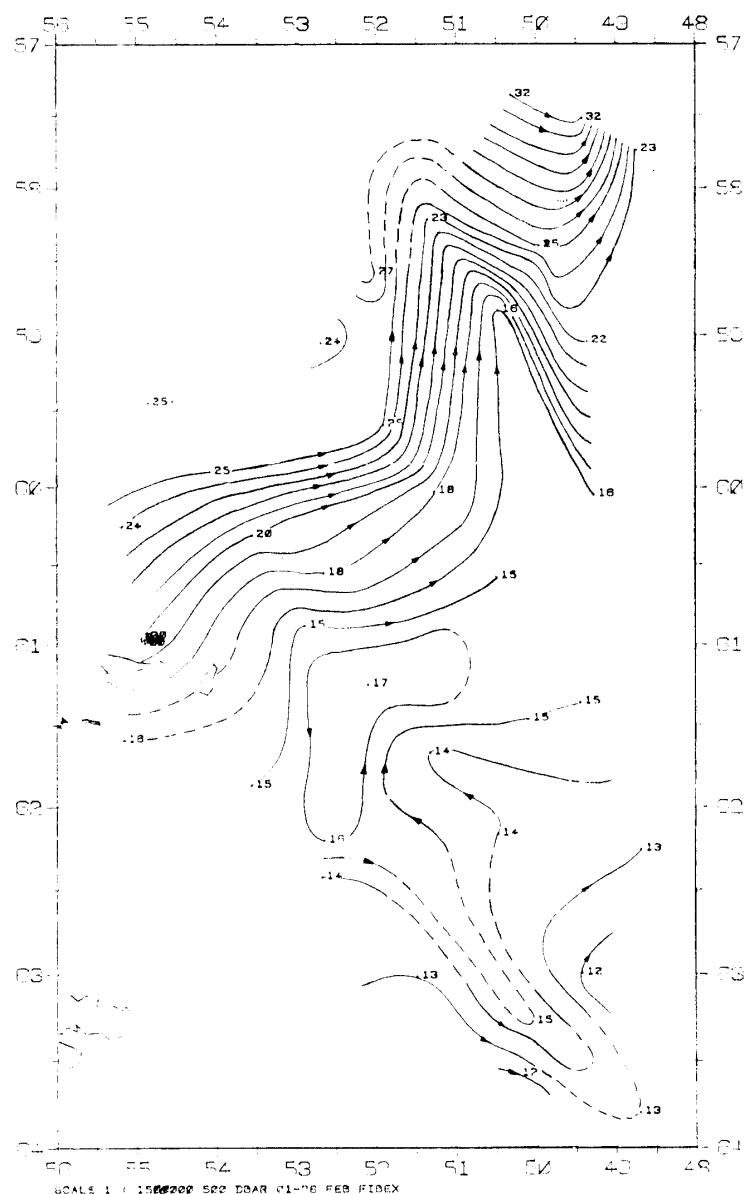


Fig. 8. Dynamic topography (dyn cm) of the 500 dbar level relative to the horizontal sea surface.

(SH_1, \dots, SH_n) and the vertical profiles of temperature (T), salinity (S) and density (σ_t) the first step to get access to the data base is to ask questions on the distribution of data in space and time. Having achieved this the program seeks out all relevant stations in the selected geographical area and time span. The program proceeds with offering an oceanographic query menu which enables answers to questions like the depth of the thermocline, dynamic topography of a given isobaric surface, watermass analysis or T, S diagrams, respectively. The individual subroutines compute the selected quantities and provide them on a geographical mapping of the area. The interpretation with isolines has to be done by the user himself.

The presentation of data was prepared for the area between 60°S and 64°S, 53°W and 63°W, covering the South Shetland archipelago, the Bransfield Strait and the north-

ern extensions of the Antarctic Peninsula as well as the southern Drake Passage. For the periods of February 15 to 28, March 1 to 14 and March 15 to 31 the relative dynamic heights (dyn cm) of the 50, 100, 200 and 500 dbar surface were plotted (Figs. 2 to 7). The plots outline the topography of the sea surface with the assumption of a horizontal 50, 100, 200 and 500 dbar surface (Fig. 8).

3. Discussion

Figures 2a, 2b, 3a and 3b delineate the kinematic situation in the southern Drake Passage during the second half of February 1981. Throughout all isobaric levels a northeasterly flow dominates the current pattern off the South Shetland Islands. The southwest going stream on the northern side of the islands (CLOWES, 1934) does not emerge in the 50 dbar and 100 dbar level during FIBEX (*cf.* Figs. 2a and 2b). Referring to the 500 dbar level (Fig. 2b) the stream-lines are roughly equidistant. This points out that the baroclinic flow between neighboring stations is very uniform north of the South Shetland Islands.

An interesting feature of the dynamic topography of the 500 dbar level is the wavy pattern of the isolines. It indicates a strong interaction between the ACC and the waters north off the South Shetland Islands.

Figures 4 to 7 represent the kinematic structure of the Bransfield Strait during March 1981. Figure a outlines the dynamic topography during the first half of the month, figure b gives the dynamic situation during the second half of March. For comparison the situation of the previous fortnight is shown in dashed lines. The characteristic flow pattern in the western parts of the strait is well demonstrated in Figs. 5a, 6a and 7a. The inflowing Bellingshausen Sea water after having passed north or south Deception Island bends to the southeast, reaches Trinity Island and turns back to the northwest before it joins the current along the south coast of the South Shetland Islands. The influence of the Weddell Sea water on the eastern parts of the strait is revealed throughout Figs. 4 to 7. Along the shore of the Antarctic Peninsula a southwesterly flow was observed (Fig. 7a) indicating the spreading of Weddell Sea water to Trinity Island, where it meets the Bellingshausen Sea water. Temporal and spatial changes of the kinematic properties are traceable in the eastern parts of the Bransfield Strait. They are predominant in the 50 dbar and 100 dbar level (Figs. 4a and 5b). The displacement of the streamlines to the west suggests the increasing influence of Weddell Sea water on the hydrographic situation of the strait during the second half of March. Combined with the increasing inflow of Weddell Sea water was an intensified drift of ice from the Weddell Sea which partly "closed" the eastern and southeastern boundary of the Bransfield Strait.

Northeast of Elephant Island the detailed structure of a Weddell-Scotia Confluence meander is visible. Whereas the current border between Pacific and Weddell Sea water masses is very broad around and north of Elephant Island the geostrophic flow is concentrating along its further way to the northeast. In the vicinity of 50°W the current border makes a characteristic bend to the southeast. As mentioned by STEIN (1981) this meander corresponds with the strong indentation of Weddell Sea water and Scotia Sea water. The flow then turns to the northeast again. In the southeastern

corner of the area a strong indentation of water masses from the South Shetland Islands shelf and from the Weddell Sea is observed.

4. Conclusion

Although there are some constraints with regard to the geostrophic method and its applicability in shallower waters this method provides us with the general circulation patterns in a very quick way. These patterns show the mean propagation of water-masses although mixing across the streamlines might occur. Since there is not any other comparable method available now and will not be in the near future we have to rely on this method for descriptive tasks. Conversion of the relative current field to an absolute current field proves not to be convenient in areas like the South Shetland Islands due to the lacking of a suitable "layer of no motion" and due to the lack of direct current measurements in this area. The value of a densely distributed set of oceanographic stations shows very impressively if one compares the conclusion made by SIEVERS (1982) with that of CLOWES (1934) and our own result. Based on the Chilean FIBEX oceanographic data set SIEVERS (1982) concludes that the typical meandering of the isolines in the Bransfield Strait does not emerge from the ITSUMI data. Unfortunately the oceanographic sections in the western part of the Bransfield Strait were just west and east of the reported meander. This supports the demand for a general FIBEX oceanographic data analysis which takes into account all data collected during FIBEX in a given area. Since this meander occurs frequently in the same region of the Bransfield Strait it is supposed here that the submarine topography between Deception Island and Trinity Island which marks the western border of the deep central basin of the strait has a steering influence on the formation and maintenance of this meander.

References

- CLOWES, A. J. (1934): Hydrology of the Bransfield Strait. *Discovery Rep.*, **9**, 1-64.
- GORDON, A. L. and NOWLIN, W. D. (1978): The basin waters of the Bransfield Strait. *J. Phys. Oceanogr.*, **8**, 258-264.
- NOWLIN, W. D., PILLSBURY, R. D. and WHITWORTH, T. (1977): Structure and transport of the Antarctic Circumpolar Current at Drake Passage from short-term measurements. *J. Phys. Oceanogr.*, **7**, 788-802.
- STEIN, M. (1978): Preliminary results of moored current meters during the German Antarctic Expedition 1977/78. *Counc. Meet. ICES, Hydrogr. Comm.*, C 5, 8 p.
- STEIN, M. (1981): Thermal structure of the Weddell-Scotia Confluence during February 1981. *Meeresforschung*, **29**(1), 47-52.
- SIEVERS, H. A. (1982): Descripción de las condiciones oceanográficas físicas, como apoyo al estudio de la distribución y comportamiento del krill. *INACH Ser. Cient.*, **28**, 87-136.

(Received November 16, 1982)